Running Cosmological Constant in light of ACT data

Bachelor thesis

Student: Mari-Ly Vijar
Student code: 223306YAFB
Supervisor: Antonio Racioppi, NICPB, senior researcher
Study program: Applied Physics

Tallinn 2026

Jooksev kosmoloogiline konstant ACT andmete valguses

Bakalaureusetöö

Üliõpilane: Mari-Ly Vijar
Üliõpilaskood: 223306YAFB
Juhendaja: Antonio Racioppi, KBFI, vanemteadur
Õppekava: Rakendusfüüsika

Tallinn 2026

Declaration

I hereby declare that I have written this thesis independently and the thesis has not previously been submitted for defence. All works and major viewpoints of the other authors, data from sources of literature and elsewhere used for writing this paper have been properly cited.

Author: Mari-Ly Vijar

The thesis complies with the requirements for bachelor's/master's theses

Supervisor: Antonio Racioppi

Abstract

In this thesis, we study a single-field inflationary model described by a logarithmic scalar potential of the form $V(\phi) = \Lambda^4[1 + \delta \ln(\phi/M)]$. The aim of the study is to analyse the inflationary dynamics of the model and to determine its predictions for the main cosmological observables.

The analysis is performed within the slow-roll approximation and focuses on the scalar spectral index n_s, the tensor-to-scalar ratio r, and the normalisation scale Λ. The parameter space is explored separately for positive and negative values of the parameter δ, as the inflationary behaviour differs qualitatively in these two cases.

For positive values of δ, the inflaton rolls down the potential and inflation ends in a standard way. The resulting observables exhibit smooth and regular dependence on the model parameters. For negative values of δ, the inflationary dynamics are more subtle. The requirement that the potential remains positive restricts the allowed field range, and the inflaton can enter and exit inflation in a non-trivial manner. Only parameter values that produce a sufficient number of e-folds lead to viable inflation.

The results demonstrate that the logarithmic inflationary potential considered in this work can give rise to consistent inflationary scenarios, while highlighting the importance of the sign of the parameter δ in determining the physical viability of the model.

Annotatsioon

Käesolevas töös uuritakse ühe skalaarväljaga inflatsioonimudelit, mida kirjeldab logaritmiline potentsiaal kujul $V(\phi) = \Lambda^4[1 + \delta \ln(\phi/M)]$. Töö eesmärgiks on analüüsida selle mudeli inflatsioonidünaamikat ning määrata selle ennustused peamiste kosmoloogiliste vaadeldavate suuruste jaoks.

Analüüs viiakse läbi aeglase rullumise *(slow-roll)* lähenduses ning keskendutakse skaalarspektri indeksile n_s, tensor-skalaar suhtele r ja normaliseerimisskaalale Λ. Parameeterruumi uuritakse eraldi parameetri δ positiivsete ja negatiivsete väärtuste korral, kuna inflatsioonikäitumine on nendel juhtudel kvalitatiivselt erinev.

Parameetri δ positiivsete väärtuste korral veereb inflaton mööda potentsiaali alla ning inflatsioon lõpeb tavapärasel viisil. Saadud vaadeldavad suurused sõltuvad mudeli parameetritest sujuvalt ja regulaarselt. Parameetri δ negatiivsete väärtuste korral on inflatsioonidünaamika keerukam. Nõue, et potentsiaal jääks positiivseks, piirab inflatoni välja lubatud vahemikku ning inflaton võib inflatsiooni käigus sellesse siseneda ja sealt väljuda mitte-triviaalsel viisil. Olulised parameetrite väärtused on ainult need, mille korral tekib piisav arv e-volte *(e-folds)*.

Tulemused näitavad, et käesolevas töös vaadeldud logaritmiline inflatsioonipotentsiaal võib viia kooskõlaliste inflatsioonistsenaariumideni, tuues esile parameetri δ märgi otsustava rolli mudeli füüsilise elujõulisuse määramisel.

Contents

1 Introduction

The Hot Big Bang framework explains many observed features of the Universe, including its expansion and the cosmic microwave background (CMB). It also raises questions related to the initial conditions of the early Universe, most notably the horizon problem and the flatness problem. The horizon problem refers to the observed near-uniform temperature of the CMB across the sky, even though, within the standard Big Bang picture, widely separated regions would not have been in causal contact before the CMB was formed. The flatness problem refers to the observation that the Universe is very close to spatially flat today, a feature that is difficult to explain within the standard Big Bang picture without fine-tuned initial conditions.

Inflation is a short phase of rapid and accelerated expansion introduced to address these issues. During inflation, a small region that was initially in causal contact is stretched to scales much larger than the observable Universe, which helps explain the observed large-scale uniformity of the CMB. At the same time, the accelerated expansion reduces the effect of any initial spatial curvature, leaving the Universe very close to spatially flat. Inflation also gives rise to observable imprints in the CMB, which are commonly summarized by the scalar spectral index $n_{\rm s}$ and the tensor-to-scalar ratio r.

By an inflationary model we mean a concrete choice of potential $V(\phi)$ for a single canonical scalar (the inflaton). There are various possible choices for V available in the literature (e.g. [1] and refs. therein). In this thesis, we study a single-field inflationary model defined by the logarithmically corrected potential

$$V(\phi) = \Lambda^4 \left[1 + \delta \ln\left(\frac{\phi}{M}\right)\right] , \tag{1}$$

also known as *running cosmological constant*. This potential can be generated by quantum corrections in a theory with several massive particles (e.g. [2] and refs. therein) and has been already applied to inflation in some specific model [3, 4, 5], where δ was not a free parameter but defined by the model itself. Instead the analysis of this thesis assumes a completely free δ, exploring both positive and negative values, and considers representative choices of the mass scale M. A positive δ naively means that the bosonic sector of the theory is more massive than the fermionic one, while a negative δ represents the opposite configuration [2]. For each case, the inflationary dynamics and the resulting observable quantities are computed at horizon exit for a fixed number of e-folds, and the model's predictions in the $(n_{\rm s}, r)$ plane are compared with current observational constraints.

2 Theory

In this section, we review the theoretical background required to study single-field inflation models and to compute the observable quantities used later in this thesis. We assume a homogeneous and isotropic Universe described by a flat Friedmann–Lemaître–Robertson–Walker (FLRW) metric.

2.1 Inflation with a scalar field

Inflation is commonly modelled by a single scalar field ϕ, called the inflaton, minimally coupled to gravity. The theoretical framework is defined by the Einstein–Hilbert action for gravity together with a canonical scalar-field action,

$$S = \int d^4x \sqrt{-g} \left[-\frac{M_{\rm P}^2}{2} R + \frac{1}{2} g^{\mu\nu} \partial_\mu \phi \, \partial_\nu \phi - V(\phi) \right], \tag{2}$$

where $g_{\mu\nu}$ is the spacetime metric, g its determinant, R is the Ricci scalar, and $M_{\rm P}$ the reduced Planck mass.

To study the cosmological evolution implied by this framework, we assume that the Universe is homogeneous and isotropic on large scales, as supported by observations. With this assumption, the spacetime geometry is uniquely described by the flat Friedmann–Lemaître–Robertson–Walker (FLRW) metric,

$$ds^2 = dt^2 - a^2(t) \left(dr^2 + r^2 d\Omega^2 \right), \tag{3}$$

where $a(t)$ is the scale factor, which describes how physical distances between comoving points evolve with time.

Varying the action in Eq. (2) with respect to the metric $g_{\mu\nu}$ yields Einstein's equations

$$G_{\mu\nu} = \frac{1}{M_{\rm P}^2} T_{\mu\nu}, \tag{4}$$

where the energy–momentum tensor of the scalar field is

$$T_{\mu\nu} = \partial_\mu \phi \, \partial_\nu \phi - g_{\mu\nu} \left[\frac{1}{2} g^{\alpha\beta} \partial_\alpha \phi \, \partial_\beta \phi - V(\phi) \right]. \tag{5}$$

For a homogeneous field $\phi = \phi(t)$ in the FLRW background, $T_{\mu\nu}$ takes the perfect-fluid form, which allows to identify the energy density and pressure as

$$\rho_\phi = \frac{1}{2} \dot{\phi}^2 + V(\phi), \qquad p_\phi = \frac{1}{2} \dot{\phi}^2 - V(\phi). \tag{6}$$

Evaluating Einstein's equations (4) for the metric (3) gives the Friedmann equations that governs the cosmic expansion. The expansion rate of the Universe is described by the Hubble parameter

$$H \equiv \frac{\dot{a}}{a}, \tag{7}$$

and the first Friedmann equation reads

$$H^2 = \frac{1}{3M_{\mathrm{P}}^2}\rho_\phi. \tag{8}$$

The acceleration equation is

$$\frac{\ddot{a}}{a} = -\frac{1}{3M_{\mathrm{P}}^2}\left(\rho_\phi + 3p_\phi\right). \tag{9}$$

Inflation is defined as a period of accelerated expansion,

$$\ddot{a} > 0. \tag{10}$$

Using Eq. (9), this condition is equivalent to

$$\rho_\phi + 3p_\phi < 0. \tag{11}$$

Substituting the expressions in Eq. (6), one finds

$$\rho_\phi + 3p_\phi = 2\dot{\phi}^2 - 2V(\phi), \tag{12}$$

so inflation occurs when the potential energy of the inflaton dominates over its kinetic energy,

$$\dot{\phi}^2 < V(\phi), \tag{13}$$

corresponding to an equation of state close to $p_\phi \simeq -\rho_\phi$.

Inflation also provides a dynamical explanation for the horizon and flatness problems of standard cosmology. It is useful to define the comoving Hubble radius as

$$(aH)^{-1}. \tag{14}$$

During accelerated expansion, the scale factor $a(t)$ grows rapidly while H varies slowly, causing $(aH)^{-1}$ to decrease. As a result, physical length scales can exit the horizon during inflation, implying that the presently observable Universe originates from a region that was initially in causal contact.

The flatness problem can be understood by including spatial curvature in the Friedmann equation

$$H^2 = \frac{1}{3M_{\rm P}^2}\rho - \frac{k}{a^2}, \tag{15}$$

which implies

$$\Omega - 1 = \frac{k}{a^2H^2}, \tag{16}$$

where $\Omega \equiv \rho/(3M_{\rm P}^2H^2)$. Since inflation causes the quantity a^2H^2 to grow rapidly, any initial deviation from spatial flatness is dynamically driven toward zero, explaining why the Universe appears nearly flat today.

Finally, varying the action (2) with respect to the scalar field yields the equation of motion for the inflaton,

$$\ddot{\phi} + 3H\dot{\phi} + V'(\phi) = 0. \tag{17}$$

2.2 Slow-roll approximation

Inflation occurs when the potential energy of the inflaton dominates over its kinetic energy. This regime is described by the slow-roll approximation, which assumes that the inflaton field evolves slowly along its potential. In this case, the dynamics can be characterised [1] by the first and second potential slow-roll parameters defined as

$$\epsilon_V(\phi) = \frac{M_{\rm P}^2}{2}\left(\frac{V'(\phi)}{V(\phi)}\right)^2, \qquad \eta_V(\phi) = M_{\rm P}^2\frac{V''(\phi)}{V(\phi)}. \tag{18}$$

The parameter ϵ_V measures the steepness of the potential and controls the rate at which inflation ends. Inflation takes place as long as $\epsilon_V \ll 1$ and $|\eta_V| \ll 1$. The end of inflation is defined by the condition

$$\epsilon_V(\phi_{\rm end}) = 1. \tag{19}$$

2.3 Number of e-folds

The amount of inflation is quantified by the number of e-folds N, which measures the growth of the scale factor during inflation. It is defined as

$$N \equiv \ln\left(\frac{a(t_{\rm end})}{a(t_*)}\right) = \int_{t_*}^{t_{\rm end}} H(t)\,dt, \tag{20}$$

where t_* denotes the time when observable modes exit the horizon and $t_{\rm end}$ corresponds to the end of inflation.[1]

[1] In order to solve the horizon and flatness problems of standard cosmology, inflation must last for a sufficiently long period, typically it's around 50-60 e-folds.

Changing the integration variable from time to the inflaton field ϕ, the expression becomes

$$N = \int_{\phi_*}^{\phi_{\rm end}} \frac{H}{\dot{\phi}}\, d\phi. \tag{21}$$

Within the slow-roll approximation, the inflaton equation of motion and the Friedmann equation simplify to

$$\dot{\phi} \simeq -\frac{V'(\phi)}{3H}, \qquad H^2 \simeq \frac{V(\phi)}{3M_{\rm P}^2}. \tag{22}$$

Using these relations, the number of e-folds can be written as

$$N \simeq \frac{1}{M_{\rm P}^2} \int_{\phi_{\rm end}}^{\phi_*} \frac{V(\phi)}{V'(\phi)}\, d\phi. \tag{23}$$

This expression allows the value of the inflaton field at horizon crossing ϕ_* to be determined once the end of inflation $\phi_{\rm end}$ is fixed by the condition given in Eq. (19).

2.4 Inflationary observables

The main observable quantities used to test inflationary models are the scalar spectral index $n_{\rm s}$ and the tensor-to-scalar ratio r. In the slow-roll approximation, these are given by

$$n_{\rm s} \simeq 1 - 6\epsilon_V^* + 2\eta_V^*, \qquad r \simeq 16\epsilon_V^*, \tag{24}$$

where the star indicates that the quantities are evaluated at $\phi = \phi_*$.

Another important observable is the amplitude of the scalar power spectrum,

$$A_{\rm s} \simeq \frac{1}{24\pi^2 M_{\rm P}^4} \frac{V_*}{\epsilon_V^*}. \tag{25}$$

The observed value of $A_{\rm s}$ can be used to fix the overall normalisation of the inflationary potential. From the constraints of the *Planck* collaboration [6], the scalar amplitude is measured to be $A_{\rm s} \simeq 2.1 \times 10^{-9}$, which provides a direct observational input for determining the energy scale of inflation in a given model.

2.5 General study of the logarithmic potential

The inflationary model studied in this thesis is defined by the logarithmically corrected potential

$$V(\phi) = \Lambda^4 \left[1 + \delta \ln\!\left(\frac{\phi}{M}\right)\right]. \tag{26}$$

Although the subsequent analysis is performed numerically, several important properties of this potential can be established analytically. These properties play a crucial role in determining the physically admissible inflationary solutions and in guiding the numerical strategy adopted later.

First, the potential must remain positive along the inflationary trajectory. Writing the potential in the form

$$V(\phi) = \Lambda^4 \, D(\phi), \qquad D(\phi) \equiv 1 + \delta \ln\left(\frac{\phi}{M}\right), \tag{27}$$

the condition $V(\phi) > 0$ is equivalent to $D(\phi) > 0$. It is convenient to introduce

$$\phi_{V=0} = M \, e^{-1/\delta}, \tag{28}$$

which defines the field value at which the potential vanishes. Requiring $D(\phi) > 0$ constrains the allowed field range in a sign-dependent manner: for $\delta > 0$, $\phi_{V=0}$ represents a lower bound on the inflaton field and physically admissible trajectories satisfy $\phi > \phi_{V=0}$, whereas for $\delta < 0$, $\phi_{V=0}$ acts as an upper bound and inflation is restricted to field values $\phi < \phi_{V=0}$.

Second, the logarithmic correction modifies the monotonicity of the potential depending on the sign of δ. Since

$$V'(\phi) \propto \frac{\delta}{\phi}, \tag{29}$$

the potential increases with the inflaton field for $\delta > 0$ and decreases with the field for $\delta < 0$. Consequently, the direction of the inflaton roll differs qualitatively between the two branches: for positive δ the field rolls toward smaller values of ϕ, while for negative δ it rolls toward larger values. This distinction becomes essential when identifying the physically relevant end of inflation.

Finally, for negative values of δ, the slow-roll parameter $\epsilon_V(\phi)$ can reach unity at two distinct values of the inflaton field. In this case, inflation is possible only within the finite field interval bounded by these two points, which correspond to the onset and termination of the slow-roll phase. As a consequence, the total number of e-folds achievable in this branch is finite, implying an intrinsic upper bound on the duration of inflation for $\delta < 0$, independent of the numerical procedure used to solve the equations of motion.

This behaviour is illustrated in Fig. 1, where $\epsilon_V(\phi)$ is shown for the representative value $\delta = -0.1$. The horizontal line $\epsilon_V = 1$ intersects the curve at two points, explicitly demonstrating the existence of a finite inflationary window in field space. Although the figure shows a specific choice of parameters, the general behaviour remains the same for different choices of the parameters if $\delta < 0$.

Parameter configurations that fail to produce a sufficient number of e-folds are therefore excluded from physical consideration.

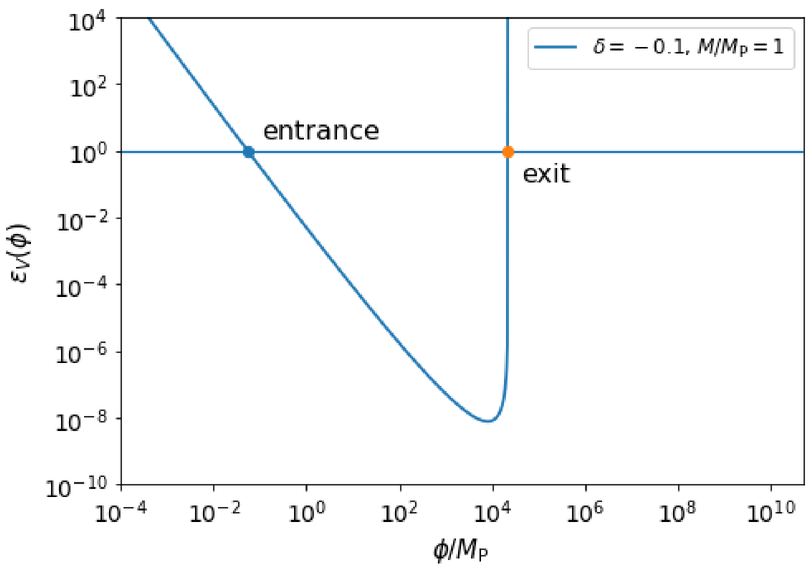

Figure 1: $\epsilon_V(\phi)$ as a function of $\phi/M_{\rm P}$ for $\delta = -0.1$ and $M = M_{\rm P} = 1$. The horizontal line shows $\epsilon_V = 1$, the two marked intersections correspond to the entry into and exit from the inflationary phase.

3 Strategy

In this section, we describe the strategy used to analyse a specific single-field inflation model characterised by a logarithmically corrected scalar potential. The potential studied in this work is given by

$$V(\phi) = \Lambda^4 \left[1 + \delta \ln\left(\frac{\phi}{M}\right)\right], \tag{30}$$

where Λ sets the overall energy scale of inflation, δ is a dimensionless parameter controlling the strength of the logarithmic correction, and M is a mass scale.

The inflationary dynamics are studied separately for positive and negative values of δ, as these two regimes exhibit qualitatively different behaviour.

3.1 Parameter ranges

The analysis is performed within the slow-roll approximation. For simplicity, the number of e-folds at horizon exit is fixed to $N_* = 55$ in order to reduce the number of free parameters and to focus on the dependence of the predictions on the model parameter δ. When presenting results in the (n_s, r) plane, the range $N_* = 50-60$ is shown to reflect the uncertainty in the total number of e-folds.

Since δ is a quantum correction, it needs to be smaller than 1. The range $|\delta| < 0.4$ was chosen since it covers all the negative δ values as can be seen in table 1.

Chosen M values are $[1, 0.1, 0.01] * M_P$

3.2 Positive δ

For positive values of δ, the potential in Eq. (30) is a monotonically increasing function of the inflaton field. As a consequence, the inflaton rolls toward smaller field values during inflation. In this case, the slow-roll parameter ϵ_V reaches unity only once, providing a unique and unambiguous definition of the end of inflation.

With the end of inflation fixed by the condition $\epsilon_V = 1$, the value of the field at horizon exit is determined from the e-fold equation given in Eq. (23). The slow-roll observables are then evaluated at horizon exit. This branch of the model does not present significant conceptual difficulties, and the analysis proceeds in a straightforward manner.

3.3 Negative δ

For negative values of δ, the inflationary dynamics are more subtle than in the positive-δ case. In this regime, the slow-roll parameter $\epsilon_V(\phi)$ may reach unity at two distinct values of the inflaton field. These two solutions correspond to the entrance into and the exit from the slow-roll phase, and only one of them represents the physically relevant end of inflation. This behaviour is illustrated in Fig. 1.

To identify the correct endpoint, the direction of the inflaton roll must be taken into account. In the slow-roll approximation, the field evolution is governed by

$$\dot{\phi} \simeq -\frac{V'(\phi)}{3H}, \tag{31}$$

which implies that the inflaton always rolls in the direction of decreasing potential. For the logarithmic potential considered here, $V'(\phi) \propto \delta/\phi$. Consequently, for $\delta < 0$ the inflaton rolls toward larger field values, while for $\delta > 0$ it rolls toward smaller field values. The physically relevant end of inflation for $\delta < 0$ is therefore given by the larger-field solution of the condition $\epsilon_V = 1$.

This behaviour is illustrated schematically in Fig. 2, which shows the potential shape and roll direction for both signs of δ.

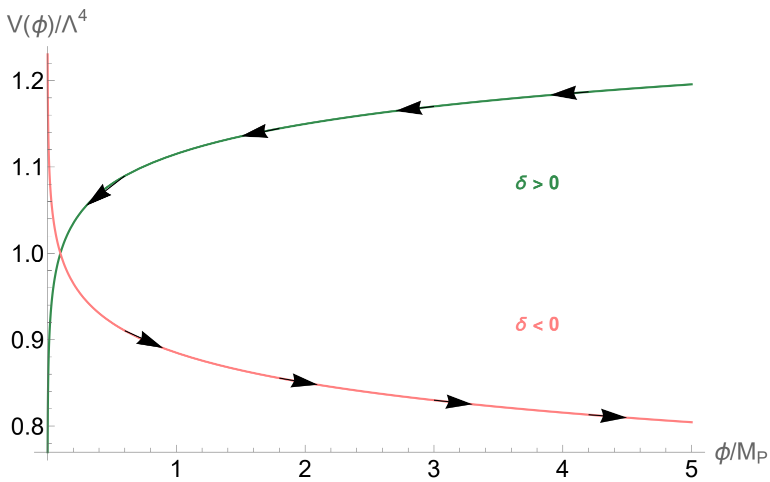

Figure 2: Illustration of the inflationary potential and inflaton roll direction for positive and negative values of δ.

In addition to the ambiguity associated with the roll direction, negative values of δ impose further consistency conditions that must be enforced in the numerical analysis. In particular, the inflationary potential must remain positive along the entire trajectory, which restricts the range of admissible field values. Furthermore, not all parameter choices lead to a sufficiently long inflationary phase: for some configurations, the maximum number of e-folds attainable between the two solutions of $\epsilon_V = 1$ is smaller than the target value $N_* = 55$. Such parameter values are therefore excluded from the analysis.

Special care is also required when computing the number of e-folds for $\delta < 0$. Although the slow-roll expression for N remains formally unchanged, the integration limits must be chosen consistently with the physical direction of the inflaton roll. Since the field rolls toward larger values of ϕ in this branch, the horizon-exit field value ϕ_* lies below the end-of-inflation value $\phi_{\rm end}$. The e-fold integral is therefore evaluated along the physical trajectory between these two points, ensuring that the resulting number of e-folds is positive and corresponds to the actual inflationary evolution.

Only those negative-δ configurations that satisfy the roll-direction criterion, maintain a positive potential throughout the trajectory, and allow for a sufficient number of e-folds are retained for the subsequent computation of inflationary observables.

4 Results

4.1 Global behaviour in the (n_s, r) plane

The overall predictions of the model in the (n_s, r) plane are shown in Fig. 3. The figure displays the trajectories obtained for different values of the mass scale M and both signs of δ, together with the observational constraints from the BICEP/*Keck* and ACT collaborations. Shaded regions indicate the 1σ and 2σ confidence levels.

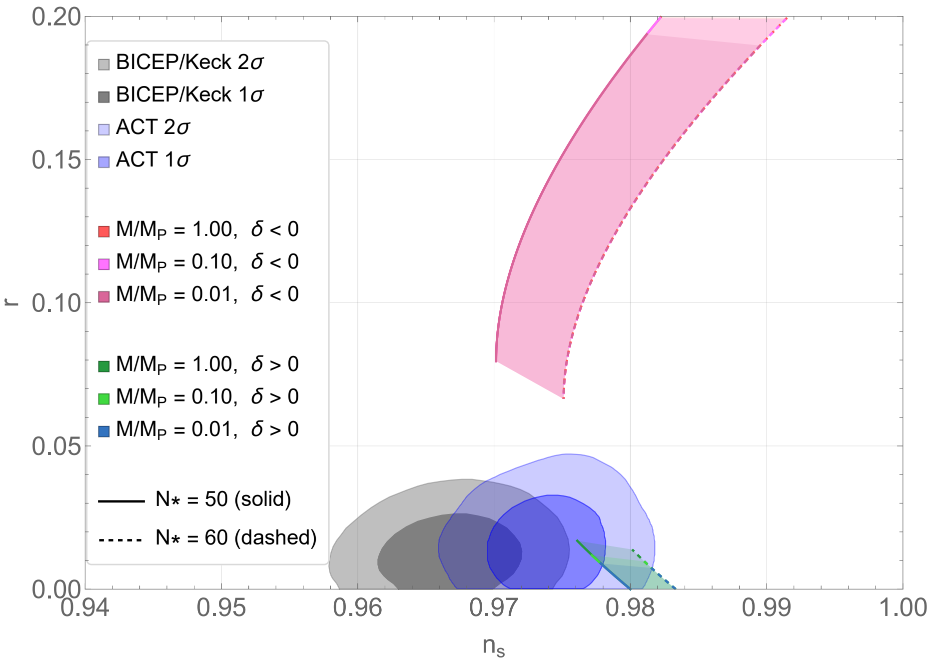

Figure 3: Model predictions in the (n_s, r) plane for positive and negative values of δ and different mass scales M. Solid and dashed lines denote $N_* = 50$ and $N_* = 60$, respectively. Shaded regions show current observational constraints.

The positive-δ branch appears in the lower part of the (n_s, r) plane, at small values of the tensor-to-scalar ratio r, with scalar spectral indices clustered around $n_s \simeq 0.98$. The trajectories are smooth and continuous as δ is varied, and their location depends moderately on the choice of the mass scale M. For suitable values of M, the positive-δ branch overlaps with the ACT confidence regions shown in the figure.

In contrast, the negative-δ branch occupies a distinct region at larger values of the tensor-to-scalar ratio r. As δ approaches zero from below, the trajectories shift toward smaller values of r; however, they remain separated from the confidence regions of BICEP/*Keck* and ACT collaborations for all mass scales considered. This separation is present for both choices of the number of e-folds shown.

4.2 Positive values of δ

For positive values of δ, the inflationary evolution proceeds along a smooth inflaton trajectory. The inflaton rolls toward smaller field values, and the slow-roll parameter $\epsilon_V(\phi)$ reaches unity only once, providing an unambiguous definition of the end of inflation. As a result, the inflationary observables vary smoothly with the model parameters.

In the remainder of this analysis, the number of e-folds is fixed to $N = 55$, a representative value within the range $N \simeq 50-60$ relevant for CMB observations. The dependence of the tensor-to-scalar ratio r on δ is shown in Fig. 4. As δ increases, the logarithmic correction steepens the potential, leading to an increase in the slow-roll parameter ϵ_V and hence to a monotonic increase in r. Throughout the explored parameter range, the predicted values of r remain relatively small.

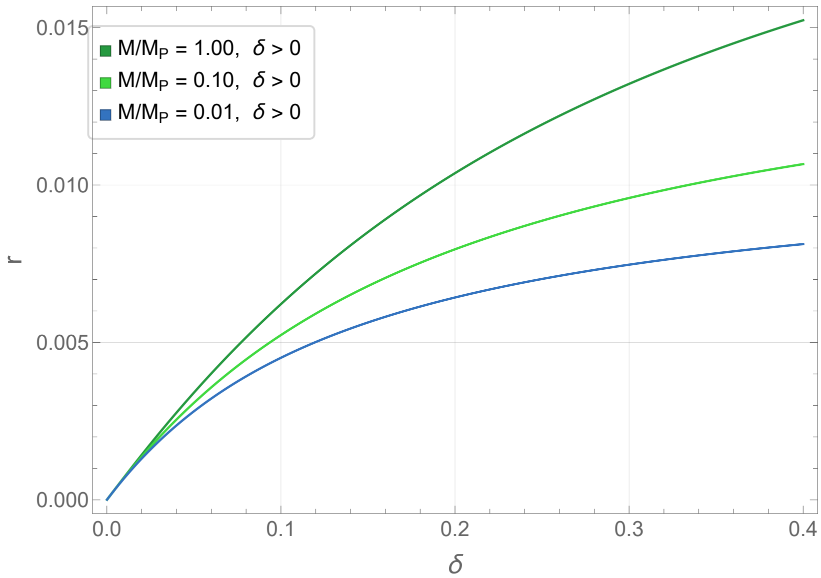

Figure 4: Tensor-to-scalar ratio r as a function of δ for $\delta > 0$.

The corresponding behaviour of the scalar spectral index is shown in Fig. 5. As δ increases, n_s decreases mildly, reflecting a gradual departure from an exactly flat plateau. This variation is smooth and remains within a narrow range for all values of the mass scale M considered.

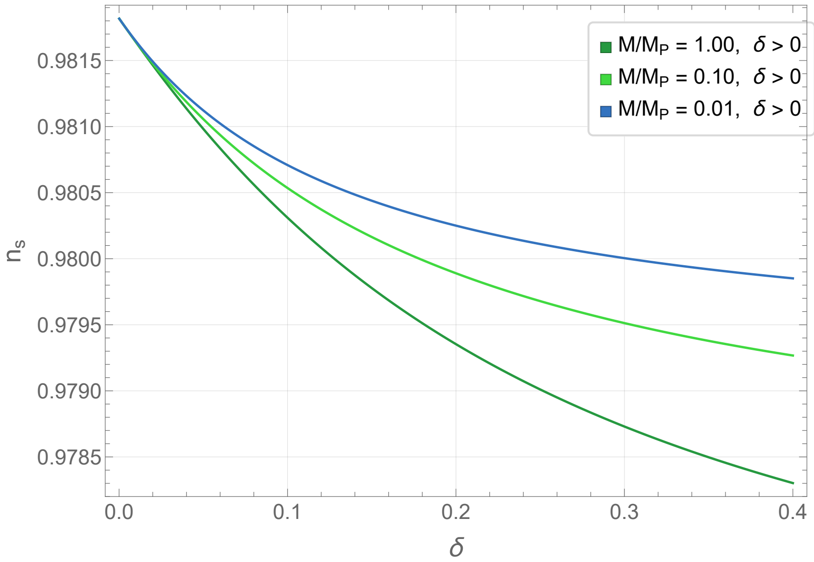

Figure 5: Scalar spectral index n_s as a function of δ for $\delta > 0$.

The inflationary energy scale Λ, fixed by matching the amplitude of the scalar power spectrum, is shown in Fig. 6. Larger values of δ require a higher inflationary scale, consistent with the increase in the slow-roll parameter ϵ_V and therefore in r.

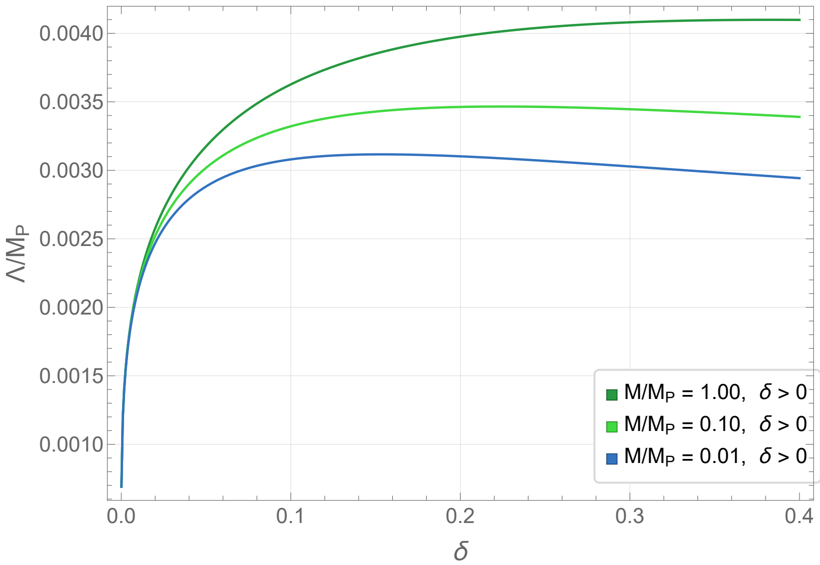

Figure 6: Inflationary energy scale Λ as a function of δ for $\delta > 0$.

Overall[2], the positive-δ branch corresponds to a plateau-like inflationary potential and leads to smooth, well-controlled predictions with low tensor-to-scalar ratios and moderate dependence on the model parameters.

[2]From the plots 4 and 5 we can see that there is an asymptotic limit for $\delta \to 0$, which is not $r = 0$ and $n_s = 1$, i.e. the results for $V = \Lambda^4$. The same applies also for the negative case.

4.3 Negative values of δ

For negative values of δ, the inflationary dynamics differ qualitatively from the positive-δ case. The inflaton rolls toward larger field values, and the slow-roll parameter $\epsilon_V(\phi)$ may reach unity at two distinct points. The physically relevant end of inflation is identified with the second crossing, corresponding to the larger value of the inflaton field.

In addition, negative values of δ impose physical constraints that restrict the viable parameter space. The potential must remain positive along the inflationary trajectory, and not all parameter choices allow a sufficient number of e-folds. Parameter configurations that fail to satisfy these conditions are excluded from the analysis. Kept delta ranges are shown in table 1.

Table 1: Kept δ ranges for the logarithmic potential model, separated by N_* and M.

N_*	M	$\delta < 0$ kept range	$\delta > 0$ kept range
50	1.0	$[-0.350304,\ -0.041791]$	$[0.0001,\ 0.4]$
50	0.1	$[-0.19388,\ -0.0381222]$	$[0.0001,\ 0.4]$
50	0.01	$[-0.133845,\ -0.0351204]$	$[0.0001,\ 0.4]$
60	1.0	$[-0.345968,\ -0.041791]$	$[0.0001,\ 0.4]$
60	0.1	$[-0.192546,\ -0.0381222]$	$[0.0001,\ 0.4]$
60	0.01	$[-0.133178,\ -0.0351204]$	$[0.0001,\ 0.4]$

The dependence of the tensor-to-scalar ratio on δ in this branch is shown in Fig. 7. Compared to the positive-δ case, the predicted values of r are significantly larger. As δ approaches zero from below, the tensor-to-scalar ratio decreases; however, it remains bounded away from the values obtained in the positive-δ branch due to the restricted inflationary dynamics.

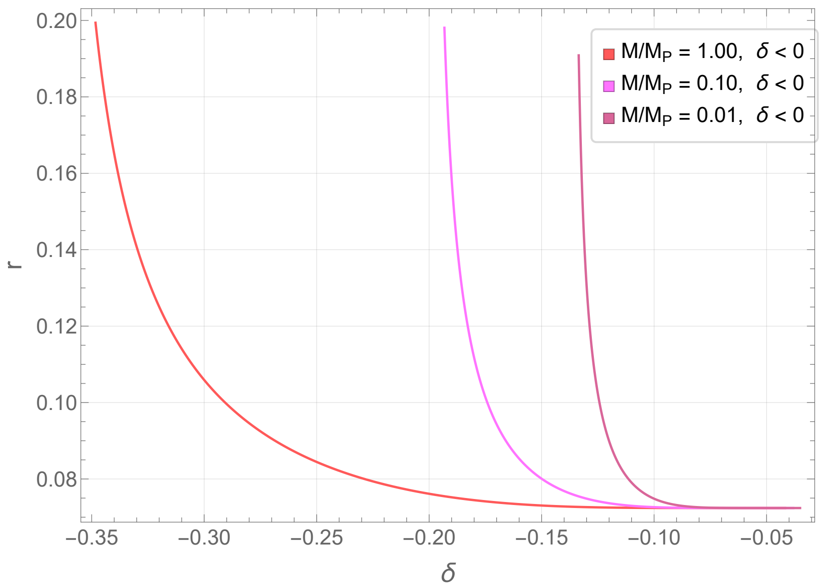

Figure 7: Tensor-to-scalar ratio r as a function of δ for $\delta < 0$.

Figure 8 shows the dependence of the scalar spectral index n_s on δ for the negative-δ branch. For each fixed value of the mass scale M, n_s varies within a relatively narrow interval when δ

is small in absolute value and changes most noticeably near the boundary of the considered δ range.

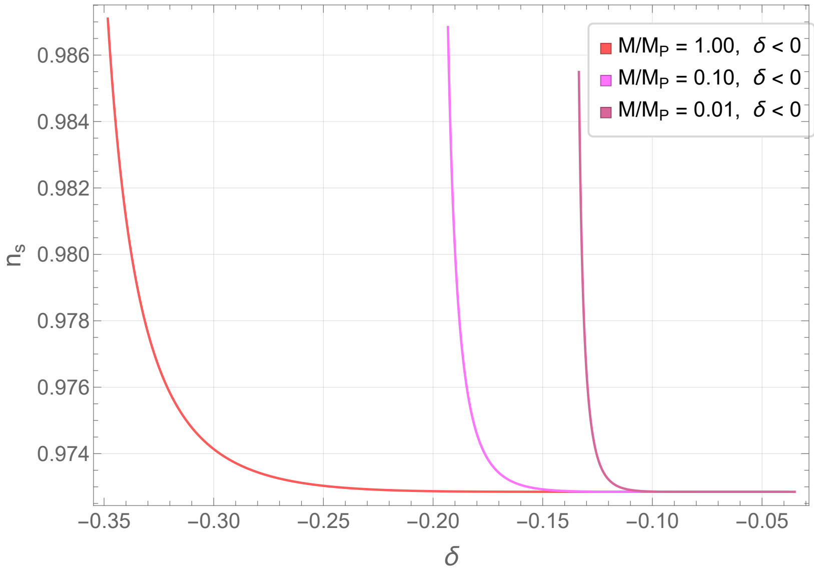

Figure 8: Scalar spectral index n_s as a function of δ for $\delta < 0$.

The corresponding inflationary energy scale is shown in Fig. 9. As δ approaches the boundary of the allowed region, the required value of Λ increases rapidly, reflecting the larger slow-roll parameter needed to reproduce the observed scalar amplitude.[3]

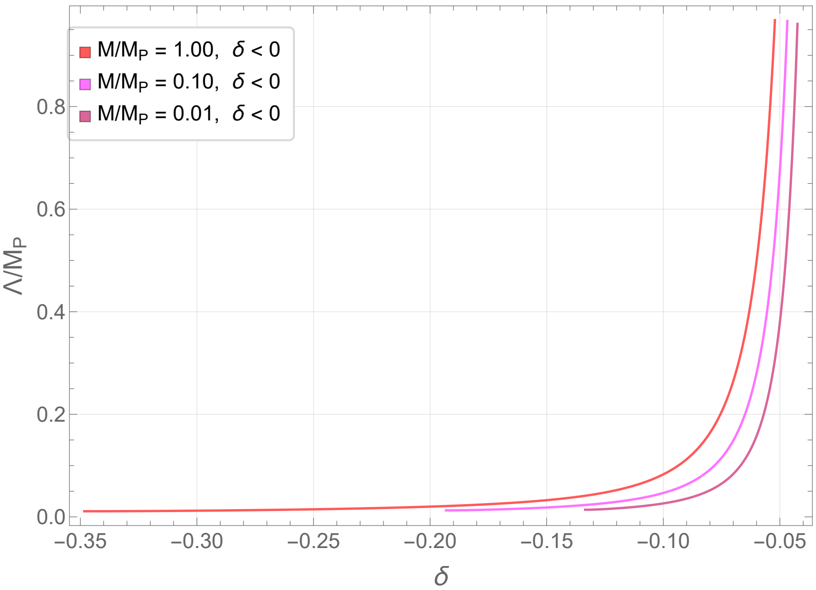

Figure 9: Inflationary energy scale Λ as a function of δ for $\delta < 0$.

[3]Due to the more complicated dynamics, in this case Λ vs δ does not have a behaviour similar to r vs. δ, in contrast to the positive δ case.

5 Conclusions

In this thesis, we analysed a single-field inflationary model defined by the logarithmic potential

$$V(\phi) = \Lambda^4 \left[1 + \delta \ln\left(\frac{\phi}{M}\right)\right],$$

with the aim of studying its inflationary predictions for both positive and negative values of the parameter δ. The analysis was carried out within the slow-roll approximation and focused on the main inflationary observables: the scalar spectral index n_{s}, the tensor-to-scalar ratio r, and the normalisation scale Λ.

For positive values of δ, the inflationary dynamics are simple and monotonic. The inflaton rolls toward smaller field values, and the slow-roll parameter ϵ_V reaches unity only once, providing an unambiguous end of inflation. In this regime, the inflationary observables depend smoothly on the model parameters. The tensor-to-scalar ratio increases monotonically with δ, while the scalar spectral index decreases slightly. The required inflationary energy scale Λ also increases with δ in order to reproduce the observed amplitude of the scalar power spectrum. In the (n_{s}, r) plane, the positive-δ branch occupies the region of small tensor amplitudes and overlaps with the observational constraints from the ACT collaboration for suitable choices of the mass scale M.

For negative values of δ, the inflationary dynamics are more constrained. The inflaton rolls toward larger field values, and the slow-roll parameter ϵ_V can reach unity at two distinct points. The physically relevant end of inflation corresponds to the second crossing, at larger ϕ. In addition, the requirement that the potential remain positive restricts the allowed field range, and not all parameter values lead to a sufficient number of e-folds. These conditions significantly reduce the viable parameter space. In this branch, the tensor-to-scalar ratio takes substantially larger values than in the positive-δ case, while the scalar spectral index varies only weakly across the allowed range. The resulting predictions remain well separated from current observational constraints in the (n_{s}, r) plane.

Overall, the logarithmically corrected inflationary potential studied in this work gives rise to two distinct branches of inflationary behaviour, determined by the sign of the parameter δ. The comparison between the two cases highlights the importance of roll direction, field-space boundaries, and consistency conditions in identifying physically meaningful inflationary solutions. These features lead to clearly separated regions in the (n_{s}, r) plane, with markedly different levels of compatibility with current observational bounds. In particular, the positive-δ branch is compatible with the CMB constraints from the ACT collaboration, whereas the negative-δ branch is largely disfavoured by the CMB constraints from the BICEP/*Keck* and ACT collaborations.

6 Acknowledgements

The author wishes to thank her supervisor, Antonio Racioppi, for his constant support and guidance, which were essential for the completion of this thesis.

References

[1] Jerome Martin, Christophe Ringeval, and Vincent Vennin. Encyclopædia Inflationaris: Opiparous Edition. *Phys. Dark Univ.*, 5-6:75–235, 2014.

[2] Ilya L. Shapiro and Joan Sola. On the possible running of the cosmological 'constant'. *Phys. Lett. B*, 682:105–113, 2009.

[3] G. R. Dvali, Q. Shafi, and Robert K. Schaefer. Large scale structure and supersymmetric inflation without fine tuning. *Phys. Rev. Lett.*, 73:1886–1889, 1994.

[4] Mansoor Ur Rehman and Qaisar Shafi. Supersymmetric hybrid inflation in light of the Atacama Cosmology Telescope data release 6, Planck 2018, and LB-BK18. *Phys. Rev. D*, 112(2):023529, 2025.

[5] Nobuchika Okada and Qaisar Shafi. Split supersymmetry and hybrid inflation in light of Atacama Cosmology Telescope DR6 data. 7 2025.

[6] Y. Akrami et al. Planck 2018 results. X. Constraints on inflation. *Astron. Astrophys.*, 641:A10, 2020.

7 Appendix 1. Non-exclusive licence

Non-exclusive licence for reproduction and publication of a graduation thesis[4]

I, Mari-Ly Vijar

1. grant Tallinn University of Technology free licence (non-exclusive licence) for my thesis "Running Cosmological Constant in light of ACT data", supervised by Antonio Racioppi,

   1.1. to be reproduced for the purposes of preservation and electronic publication of the graduation thesis, incl. to be entered in the digital collection of the library of Tallinn University of Technology until expiry of the term of copyright;

   1.2. to be published via the web of Tallinn University of Technology, incl. to be entered in the digital collection of the library of Tallinn University of Technology until expiry of the term of copyright.

2. I am aware that the author also retains the rights specified in clause 1 of the non-exclusive licence.

3. I confirm that granting the non-exclusive licence does not infringe other persons' intellectual property rights, the rights arising from the Personal Data Protection Act or rights arising from other legislation.

05/01/2026

[4] The non-exclusive licence is not valid during the validity of access restriction indicated in the student's application for restriction on access to the graduation thesis that has been signed by the school's dean, except in case of the university's right to reproduce the thesis for preservation purposes only. If a graduation thesis is based on the joint creative activity of two or more persons and the co-author(s) has/have not granted, by the set deadline, the student defending his/her graduation thesis consent to reproduce and publish the graduation thesis in compliance with clauses 1.1 and 1.2 of the non-exclusive licence, the non-exclusive licence shall not be valid for the period.